Published in final edited form as:
Biochemistry. 2011 August 23; 50(33): 7117–7131. doi:10.1021/bi200905x.

Efficient isolation of *Pseudomonas aeruginosa* type III secretion translocators and assembly of heteromeric transmembrane pores in model membranes†

Fabian B. Romano[II,*], **Kyle C. Rossi**[II], **Christos G. Sava**[§], **Andreas Holzenburg**[§,⊥,#], **Eugenia M. Clerico**[II], and **Alejandro P. Heuck**[II,*,‡]

[§]Microscopy and Imaging Center, Texas A&M University, College Station, TX 77843, USA

[⊥]Department of Biology, Texas A&M University, College Station, TX 77843, USA

[#]Department of Biochemistry and Biophysics, Texas A&M University, College Station, TX 77843, USA

[II]Department of Biochemistry and Molecular Biology, University of Massachusetts, Amherst, MA 01003, USA

[*]Program in Molecular and Cellular Biology, University of Massachusetts, Amherst, MA 01003, USA

Abstract

Translocation of bacterial toxins or effectors into host cells using the Type III Secretion (T3S) system is a conserved mechanism shared by many Gram-negative pathogens. *Pseudomonas aeruginosa* injects different proteins across the plasma membrane of target cells altering the normal metabolism of the host. Protein translocation presumably occurs through a proteinaceous transmembrane pore formed by two T3S secreted protein translocators, PopB and PopD. Unfolded translocators are secreted through the T3S needle prior to insertion into the target membrane. Purified PopB and PopD form pores in model membranes. However, their tendency to form heterogeneous aggregates in solution had hampered the analysis of how these proteins transition from a denatured state to a membrane-inserted state. Translocators were purified as stable complexes with the cognate chaperone PcrH, and isolated from the chaperone using 6 M urea. We report here the assembly of stable transmembrane pores by dilution of urea-denatured translocators in the presence of membranes. PopB and PopD spontaneously bound liposomes containing anionic phospholipids and cholesterol in a pH dependant manner as observed by two independent assays, time-resolved FRET and sucrose-step gradient ultracentrifugation. Using Bodipy-labeled proteins we found that PopB interacts with PopD on the membrane surface as determined by excitation energy migration and fluorescence quenching. Stable transmembrane pores are more efficiently assembled at pH lower than 5.0, suggesting that acidic-residues might be involved in the initial

[†]This research was supported by a Biomedical Research Grant from the American Lung Association and the Massachusetts Thoracic Society to A.P.H.. F.B.R. was partially supported by National Research Service Award T32 GM08515 from the National Institutes of Health. K.C. R. was a recipient of the HHMI Undergraduate Science Program Summer Research Internship.

[‡]Corresponding Author: Dr. Alejandro P. Heuck, 710 N. Pleasant St., Lederle GRT Rm 816, University of Massachusetts, Amherst, MA 01003, Phone: (413) 545-2497, Fax: (413) 545-3291, heuck@biochem.umass.edu.

SUPPORTING INFORMATION AVAILABLE

Details on cloning expression and purification of proteins; aggregation of hisPcrH-PopB; PopB and PopD site-directed mutagenesis; SEC analysis of homogeneous chaperone-translocator complexes; pH dissociation vs urea dilution activities at pH 5.1; intermolecular disulfide formation by hisPcrH, pH solubility of hisPcrH-PopD; steady state FRET for protein-membrane binding; particle size analysis by DLS, and lifetime analysis for time-resolved FRET efficiencies. This material is available free of charge via the Internet at http://pubs.acs.org.

membrane binding and/or insertion. Altogether, the experimental setup described here represents an efficient method for the reconstitution and analysis of membrane-inserted translocators.

Transport of proteins across membranes is essential at many stages of pathogen infection and colonization of human cells. This process is important to discharge the proteins outside the pathogenic organism (secretion), and to introduce these secreted toxins/effectors into the cytosol of the target cell (translocation). Many pathogens including *Shigella*, *Salmonella*, *Yersinia* and *Pseudomonas* species, exploit a sophisticated and efficient mechanism of toxin secretion and translocation known as the type III secretion (T3S) system (1–3). It is well known that *P. aeruginosa* pathogenesis depends on a vast arsenal of virulence factors including the T3S system, which is a key factor for acute infections (4, 5). The T3S system is a syringe-like macromolecular secretion system formed by more than 20 different proteins organized into three major structures to span: i) the inner bacterial membrane, the periplasmic space, the outer bacterial membrane (*secreton*); ii) the extracellular space (*needle*); and iii) the host cellular membrane (*translocon*). Great progress has been made in the structural characterization of the secreton and the needle in related organisms (6). However, virtually nothing is known about how T3S secreted proteins are translocated across the plasma membrane of the target cell (7). Some genetic and biochemical evidence suggest that effector proteins are translocated across the host plasma membrane through a proteinaceous pore or translocon formed by two bacterial secreted proteins (the translocon hypothesis) (7–9).

The translocon hypothesis states that the *P. aeruginosa* T3S translocators, PopB and PopD, insert into the target membrane, engage with the tip of the T3S needle (formed by PcrV 10), and assist translocation of effector proteins into the host cell. The hypothesis is based on the following experimental observations i) PcrV, PopB and PopD are not required for effector secretion, but are essential for effector translocation into the target cell (11–13), ii) only PopB and PopD are found inserted into the target membrane after pathogen-host contact (13), iii) PcrV, PopB and PopD are necessary to observe T3S dependent cell lysis (11, 13, 14), and iv) PopB and PopD can form pores in model membranes either individually or in combination (15, 16).

Current models for the *P. aeruginosa* translocon complex are quite rudimentary, and they are based in the following observations: i) the translocon proteins PopB and PopD are found associated with cell membranes after the interaction of *P. aeruginosa* with red blood cells (13); ii) PopB co-immunoprecipitates with PopD after Triton X-100 solubilization of membrane associated proteins (13); and iii) ring-like structures are observed using electron microscopy when the translocon proteins are incubated with model membranes (15). The topology of the translocon proteins is based only on the bioinformatic analysis of the primary structure for these proteins, which suggests that PopB possesses two potential transmembrane (TM) segments and PopD only one (8), but no experimental data are available to corroborate such predictions. The non-polar character of the T3S translocators and their tendency to aggregate in solution has made the structural and functional characterization of these proteins very difficult (17, 18).

We have purified and characterized the *P. aeruginosa* translocators individually as homogeneous complexes with the cognate chaperone PcrH. After isolation, PopB and PopD were quantitatively separated from PcrH by combining immobilized metal ion affinity chromatography (IMAC) and elution with the chaotropic agent urea. The spectroscopic characterization of the urea-isolated PopD showed little secondary structure content, and that the two Trp residues were exposed to a polar environment. In contrast, the urea-isolated PopB presented more alpha helical content than PopD, and its single Trp residue was located in a non-polar environment. The pore forming activity of the urea-isolated translocators was

very similar to the activity of the translocators separated from the chaperone by acidification (16). Assembly and maximal pore formation occurred at pH below 5, indicating that protonation of acidic residues was critical for membrane insertion. Under these conditions, PopD, PopB, and their mixtures formed discrete and stable pores in lipids vesicles. Cryo-electron microscopy (EM) and dynamic light scatter (DLS) revealed that no aggregation or disruption of the integrity of the vesicles occurred after assembly of the transmembrane pores. Single Cys residues were introduced at specific locations in PopD and PopB, and these derivatives purified and labeled with the fluorescent probe Bodipy. Using both Bodipy excitation energy migration and self-quenching, we unambiguously showed that PopB interacts with PopD on lipid membranes. We have therefore established an efficient procedure to purify, specifically label, and assemble the *P. aeruginosa* translocators and their derivatives into model membranes.

EXPERIMENTAL PROCEDURES

Expression and Purification of proteins

The expression and purification of the hisPcrH, hisPcrH-PopD, hisPcrH-PopB, and derivatives were done as described in supporting information. The protein concentration was estimated using molar absorptivity of 18,910 $M^{-1}cm^{-1}$ for hisPcrH, 13,980 $M^{-1}cm^{-1}$ for PopD, 6,990 $M^{-1}cm^{-1}$ for PopB (19), and assuming 1:1 chaperone-translocator complexes.

Isolation of PopB and PopD using 6 M urea

2–4 mg of purified hisPcrH-PopD (or hisPcrH-PopB) were loaded onto spinTrap IMAC columns (GE Healthcare) packed with 300 μl each of Quelating Sepharose Fast Flow (GE Healthcare) resin slurry, previously loaded with Co^{2+} and equilibrated with buffer A. [20 mM 2-Amino-2-hydroxymethyl-propane-1,3-diol (Tris-HCl), pH 8.0, 100 mM NaCl]. Elution of PopB or PopD through the resin took place by spinning dry the columns for 30 sec at 2000×g. 450 μl of buffer B (Tris-HCl 20mM pH 8.0) supplemented with 6 M urea and 20 mM Gly, was added and columns were incubated for 30 min at 4°C on a rocking platform. Dissociated PopD (or PopB) were eluted by spinning the columns for 30 sec at 2000×g. Samples were fractionated, frozen in liquid N_2 and storage at −80°C until use.

Mass Spectrometry

Purified PopB and PopD were analyzed using an Esquire Mass spectrometer (Brucker Daltonics, Billerica, MA) equipped with electro-spray ionization source and ion-trap mass detector. 0.1 mg of protein was dialyzed extensively against pure water at 4°C. Then, protein was diluted to 50% v/v methanol, 3% acetic acid and sprayed intro the ionization source at a 120 μl/hr rate. Mass/charge data was collected, averaged, and protein molecular mass was calculated from deconvolution of the average mass spectra.

Fluorescent protein labeling

$PopB^{S164C}$ (introduced mutations are indicated using a superscript text where the substituted amino acid and the introduced amino acid are indicated at the left and the right side of the number, respectively) and $PopD^{F223C}$ were labeled using N-(4,4-difluoro-5,7-dimethyl-4-bora-3a,4a-diaza-s-indacene-3-yl)methyl)iodoacetamide (Bodipy FL C_1-IA or Bodipy, Invitrogen) as follows. Two mg of $PopB^{S164C}$ or $PopD^{F223C}$ complexed with hisPcrH were first incubated in buffer A supplemented with 5mM DTT for 1 hr, then run through a Sephadex G-25 column (1.5 cm I.D. × 20 cm) pre-equilibrated with buffer C (Hepes 50 mM pH 8.0, 100 mM NaCl). Given the relatively low water solubility of Bodipy, dye dissolved in dymethyl sulfoxide was added in four consecutive steps to the protein solution with a 5:1 dye:protein ratio each. The first two additions were followed by 1 hr incubation at 20–23°C

in the dark with gentle shaking, while the last two additions were followed by a 30 min incubation in same conditions. Then, any precipitated dye and protein were cleared out by centrifugation and excess soluble fluorophore was removed by SEC using Sephadex G-25 resin pre-equilibrated with buffer Tris 20 mM pH 7.5, 100 mM NaCl. $PopB^{S164C\text{-}Bodipy}$ and $PopD^{F223C\text{-}Bodipy}$ were isolated from hisPcrH using urea 6 M as described for wild type translocators. The non-lytic, pre-pore former Perfringolysin O derivative ($PFO^{E167C\text{-}F181A\text{-}F318A\text{-}C459A}$ or PFO) was labeled with Bodipy as indicated above for the translocators. Labeling efficiencies were calculated as 96% for $PopD^{F223C\text{-}Bodipy}$, 68% for $PopB^{S164C\text{-}Bodipy}$, and 100% for PFO^{Bodipy} by using the molar absorptivities at 280nm for PopB and PopD (see above), PFO (20), and Bodipy (55,000 cm^{-1} M^{-1} at 502 nm in 6M urea). The absorbance of Bodipy at 280 nm was ~4% of the absorbance at 502 nm.

Liposome Preparation

All non-sterol lipids were obtained from Avanti Polar Lipids (Alabaster, AL). Cholesterol was obtained from Steraloids (Newport, RI). Liposomes were generated using an Avanti® Mini-Extruder (Alabaster, AL) and polycarbonate filters with a 0.1 μm pore size (Whatman) as described previously (21). Briefly, a mixture of 1-palmitoyl-2-oleoyl-*sn*-glycero-3-phosphocholine (POPC), Cholesterol, and 1-palmitoyl-2-oleoyl-*sn*-glycero-3-phosphoserine (POPS) (65:20:15 mol %, respectively) in chloroform was dried at 20–23°C under N_2 and then kept under vacuum for at least 3 hrs. Lipids were hydrated by adding buffer C to a 10–30 mM final concentration of total lipids, and incubated for 30 min at 20–23°C with vortexing at 5 min intervals. The suspended phospholipid/sterol mixture was frozen in liquid N_2 and thawed at 37 °C a total of three cycles to reduce the number of multilamellar liposomes and to enhance the trapped volumes of the vesicles. Hydrated lipids were extruded 21 times through a 0.1 μm pore size polycarbonate filter. All liposome preparations were analyzed as monodisperse with an average particle diameter of about 100 nm +/− 5 nm by using DLS. The resultant liposomes were stored at 4°C and used within 2 weeks of production. Liposomes used in FRET experiments were prepared similarly, except that 0.5 mol % of the total lipid was replaced with rhodamine B 1,2-dihexadecanoyl-sn-glycero-3-phosphoethanolamine (Rh-PE), triethylammonium salt (Invitrogen). The pore forming activity of translocators was measured using liposomes containing $Tb(DPA)_3^{3-}$. The $Tb(DPA)_3^{3-}$ loaded liposomes were prepared as described previously by us (22).

Liposome Flotation –Membrane Binding Assay

Binding reactions (75 μl) containing liposomes (2 mM total lipids) and Bodipy-labeled PopB or PopD (400 nM total protein) were established in ultracentrifuge tubes and incubated at 20–23°C for 1 hr. Binding reaction buffer was a mixture of sodium acetate 30 mM and 2-(*N*-morpholino)ethanesulfonic acid 30 mM regulated at pH 4.0 or 6.0. Liposomes were equilibrated with the buffer prior to protein addition. Liposome-bound and unbound proteins were separated by flotation of proteoliposomes through a sucrose gradient as follows. A 225 μl aliquot of 67% sucrose was thoroughly mixed with each binding reaction and the samples were overlaid with 360 μl of 40% sucrose, followed by 240 μl of 4% sucrose. Samples were centrifuged for 50 min at 90,000 × g at 4 °C (23). Three 300 μl fractions (upper fraction containing proteoliposomes, middle fraction empty, and bottom fraction containing free protein) were collected from the gradient. After trichloroacetic acid precipitation and resuspension in SDS denaturalization buffer, samples were analyzed by SDS-PAGE followed by fluorescence scan using a FLA-500 phosphorimager (Fujifilm Corporation, Japan). Protein bands corresponding to liposome bound protein were quantified by gel densitometry using Genetools 4.01 software (Syngene, UK).

Dynamic light scattering

Unless otherwise indicted the average size of the liposomes was determined at 20–23°C using a PDDLS Coolbatch/PD2000DLS instrument (Precision Detectors, Inc., Franklin, MA) employing a 30 mW He-Ne laser source (658 nm) and a photodiode detector at an angle of 90°. Average autocorrelation functions were fit using the cumulant method and hydrodynamic radius derived from the obtained decay rates (24).

Cryo-EM

Samples were prepared for cryo-EM by applying 3 μl of the liposome-protein mixture to freshly glow-discharged holey carbon films (C-Flat, Protochips Inc.) and plunge freezing them in liquid ethane using an FEI Vitrobot. Specimens were observed on an FEI Tecnai F20 transmission electron microscope operating at 200 kV. Images were acquired under low-dose and zero-loss imaging conditions on a Gatan Ultrascan 1000 attached to the end of a Gatan Tridiem post-column energy filter.

Pore Formation Assay

Liposomes were suspended to a final concentration of 0.15–0.30 mM total lipids in 300 μl of buffer D (sodium acetate 50 mM pH 4.0, 5 mM EDTA). The net initial emission intensity (F_0) was determined after equilibration of the sample at 25°C for 5 min. Aliquots of PopB or PopD were added to the liposome suspension at a 30–60 nM concentration and samples were incubated 15 min at ~23°C. After re-equilibration to 25°C, the final net emission intensity (F_f) of the sample was determined (i.e., after blank subtraction and dilution correction) and the fraction of $Tb(DPA)_3^{3-}$ quenched was estimated using $(F_0\text{-}F_f)/F_0$ (22). For the analysis of the pore forming activity at different pHs, an equimolar mixture of sodium acetate 30 mM and 2-(*N*-morpholino) ethanesulfonic acid 30 mM was used.

Analysis of formed pores

The presence of discrete size membrane pores formed by PopB, PopD, or an additive equimolar mixture of both was estimated by measuring the ability of biocytin (~1.5 nm size) or biotin-β-amylase (~4 nm size) to diffuse through the pores formed by translocators. Liposomes encapsulating streptavidin^{Bodipy} were treated with the translocator/s and diffusion of the biotin markers through the pores was detected as an increase in streptavidin^{Bodipy} fluorescence as follows: liposomes loaded with streptavidin^{Bodipy} (100 μM total lipids) were suspended in buffer sodium acetate 50 mM pH 4.3, 0.5 mM DTT, containing 1 μM biocytin or 100 nM biotin-β-amylase. The net initial emission intensity (F_0) was determined after equilibration of the sample at 25°C for 5 min. Translocators were added individually or together at a final concentration of 100 nM each and samples were incubated at 20–23°C for 15 min (protein:lipid ratio 1/1000 for individual proteins, and 1/500 when both proteins were added together). After re-equilibration at 25°C the final net emission intensity (F) of the sample was determined (i.e., after blank subtraction and dilution correction) and the enhancement of streptavidin^{Bodipy} fluorescence emission was estimated using (F/F_0), which is proportional to the amount of biotinylated marker able to diffuse through membrane pores and bind to streptavidin^{Bodipy}. As a control, samples containing biotin-β-amylase were treated with Triton X-100 after recording F in order to disrupt membranes and corroborate the binding activity between biotin-β-Amylase and streptavidin^{Bodipy} (not shown).

Circular dichroism (CD) spectrosopy

Measurements were performed at 25°C on a Jasco J-715 spectropolarimeter (Jasco Corporation, Japan) equipped with a Peltier-effect device for temperature control. Scan speed was set to 20 nm/min with a 1 sec response time, 0.5 nm data pitch and 1 nm

bandwidth. Far-UV spectra were collected using 0.2 cm cells and protein concentration 2–3 μM in buffer E (sodium phosphate 10 mM, pH 7.5). Six spectra were recorded and averaged for each sample.

Steady-State Fluorescence Spectroscopy

Steady-state fluorescence measurements were collected using a Fluorolog-3 photon-counting spectrofluorimeter equipped with a double monochromator in the excitation light path, a single emission monochromator, cooled photo multiplier tube housing, and a 450 W xenon lamp and temperature controlled sample holder (20). For pore formation activity assays employing $Tb(DPA)_3^{3-}$ liposomes, excitation/emission wavelengths were set to 278/544 nm and a 385 nm long pass filter was placed in the emission channel in order to block second-order harmonic light from passing through the emission monochromator. The bandpass was typically 2 nm for excitation and 4 nm for emission. For experiments using streptavidin-Bodipy samples were excited at 492 nm and the emission intensity was measured at 510 nm. Emission scans of intrinsic protein fluorescence were carried out at 1 nm intervals between 285 and 405 nm, excitation wavelength was 278 nm. Emission scans for FRET experiments were carried out at 1 nm intervals between 490 and 560 nm, excitation wavelength was 485 nm.

Time-Resolved Fluorescence Spectroscopy

Time-resolved fluorescence measurements were carried out in a Chronos multifrequency cross-correlation phase and modulation fluorometer equipped with a three chamber cuvette holder for background subtraction from ISS (Champaign, IL). Samples were excited with a 470 nm laser diode (HBW 4 nm) filtered through a 472 nm interference filter (transmittance % HBW 10 nm) to eliminate spurious light. Emitted light was collected through a Melles Griot GG 495 sharp cutoff glass filter to eliminate scattered light and a Melles Griot 03SWP608 dielectric shortpass filter at 550 nm to minimize the contribution of direct excitation of Rh-PE. To avoid any polarization artifacts, measurements were done under magic angle conditions using Glan-Thompson Prism Polarizers (10×10 mm aperture in the excitation, and 14×14 mm aperture in the emission, set at 0° and 55° relative to the lab vertical axis, respectively). Fluorescence lifetimes were calculated by measuring the phase delay and modulation ratio spectra of samples in the 10 to 200 MHz frequency modulation range selecting 25 frequencies (25°C). Blank subtraction was carried out using an equivalent sample without the fluorophore and using the algorithm described by Reinhart et al (25) incorporated into the acquisition software. A solution of Fl (Invitrogen) in NaOH 0.1 M was used as a reference lifetime with a value of 4.05 ns (21, 26), and a total intensity similar to the one of the measured sample (±10 %) (27). One single exponential lifetime of 4.05 ± 0.1 ns was obtained for this reference sample when measured against rhodamine B in methanol (lifetime 2.5 ns, 28). The lifetime data were analyzed assuming different models including monoexponential, multiexponential, or continuous lifetime distribution (29) decay models. The goodness of the fit was determined by using the reduced χ^2 values. Uncertainties in the phase and modulation values were considered 0.2 and 0.004, respectively.

Membrane binding FRET measurements

The binding of $PopB^{S164C\text{-}Bodipy}$ or $PopD^{F223C\text{-}Bodipy}$ to membranes under equilibrium conditions was measured by Förster resonance energy transfer (FRET) between a Bodipy-labeled translocator (donor or D), and Rh-PE as acceptor (A), randomly distributed at the lipid bilayer. Four biochemically equivalent samples were prepared in parallel: sample D_o (D only) contained 120 nM total translocator (an equimolar mixture of Bodipy-labeled translocator mutant and wild type translocator was used to minimize Bodipy self-quenching), and POPC:POPS:cho membranes (65:15:20 molar ratio) lacking Rh-PE; sample DA (D plus A) contained the same protein mixture as in D_o and membranes containing Rh-

PE (0.5% of the total lipids); sample A_o (A only) contained 120 nM wild type translocator and vesicles containing Rh-PE; and the blank (B) sample contained 120 nM wild type translocator and vesicles lacking Rh-PE. In all four samples, the total lipid concentration of the membranes was 0.3 mM. All samples were incubated at 25°C for 30 min to permit complete insertion of translocator derivatives to the model membranes before spectral measurements at 25°C. FRET efficiency (*E*) was calculated as describe by Wu & Brand (30)

$$E=1-\left(\frac{\langle\tau_{DA}\rangle_a}{\langle\tau_D\rangle_a}\right)$$

where τ_{DA} and τ_D are the average amplitude weighted lifetimes of the D in the presence and absence of A, respectively. The τ_{DA} and τ_D for DA and D_o samples were determined as described in the time-resolved fluorescence spectroscopy section using the A_o and B samples for blank subtraction, respectively. Phase-delay and modulation-ratio data best fit to two-exponential component models.

RESULTS

Purification of homogeneous chaperone-translocator complexes containing native PopB and PopD

Co-expression of hisPcrH with native PopD (or PopB) was achieved by using the pETDuet-1 system (Merk4Biosciences) as described under Experimental Procedures. The translocators were therefore purified in their native state, without modifications (i.e., no affinity tags or amino acid additions/deletions resulting from the cloning procedure into the expression vector). The absence of polyHis tags or fusion-proteins (e.g., GST) is critical when electrostatic interactions and oligomerization of proteins are involved in the mechanism under investigation. Water-soluble hisPcrH-PopD and hisPcrH-PopB complexes were purified using IMAC and AEC. The IMAC step rendered a mixture of free hisPcrH together with hisPcrH-PopD (or hisPcrH-PopB) complexes (not shown). The AEC step separated the free hisPcrH chaperone and other minor contaminants from the hisPcrH-PopD (or from the hisPcrH–PopB) complex (Fig. 1A and 1B). A major peak containing the hisPcrH-PopD complex eluted when the concentration of NaCl was 0.21 M. The free hisPcrH chaperone eluted later when the concentration of NaCl was 0.35 M (Fig.1A).

Size exclusion chromatography (SEC) analysis of the purified hisPcrH-PopD complex revealed a single symmetric peak (Fig. S1). When compared to the elution times of molecular mass standards, hisPcrH-PopD eluted with an apparent molecular mass of 111 ± 1 kDa (expected 50.8 kDa), which suggested that hisPcrH-PopD may form 2:2 complexes. Similar SEC results have been described for *Shigella flexneri* (31) and *Aeromonas hydrophila* (32) translocators, however analysis of these complexes have shown they adopt a 1:1 stoichiometry. Therefore it seems that purified hisPcrH-PopD forms an elongated 1:1 complex, as described for the *P. aeruginosa* CHA translocator and other related T3S proteins (15, 31, 32).

In contrast to hisPcrH-PopD, the hisPcrH-PopB complex eluted in two peaks during the AEC step (Fig. 1B). The first peak eluted at 0.19 M NaCl and a second peak eluted at 0.25 M NaCl. A third peak corresponding to the free hisPcrH chaperone eluted at a higher NaCl concentration (~0.30 M). SEC analysis of isolated fractions from the peaks revealed that the first peak corresponded mainly to a 1:1 hisPcrH-PopB complex (eluted at 13.9 mL), while the second peak contained a larger proportion of aggregates (Fig. 1C). Interestingly, we noticed that the amount of hisPcrH-PopB appearing as aggregates was affected by the

concentration of the proteins (Fig. S2B). The higher the protein concentration of the sample, the larger the amount of non-specific hisPcrH-PopB aggregates observed, confirming the intrinsic tendency of the complex to aggregate in aqueous solution (15, 32).

The hisPcrH-PopB peak corresponding to the 1:1 complex was isolated and reanalyzed by SEC. A main symmetric peak eluted in the second SEC run (Fig. S1), indicating that hisPcrH-PopB was stable in solution and ran with a hydrodynamic radius equivalent to a globular protein of 95 ± 3 kDa. Since the expected molecular weight for a 1:1 complex is 59.6 kDa, this result suggested that hisPcrH-PopB adopted an elongated conformation rather than a globular shape, as shown previously for the homologue protein AopB (32).

We have therefore optimized the procedures to obtain both hisPcrH-PopD and hisPcrH-PopB complexes purified to apparent homogeneity (Fig. 1D, lanes 2 and 3, and Fig S1).

Spectroscopic and functional characterization of the purified chaperone associated proteins

The far-ultraviolet (UV) CD spectrum of the purified chaperone hisPcrH revealed a typical all-α protein, with double minima around 222 nm and 209 nm (Fig. 2A). These data correlated well with the recently solved three dimensional structure of the $PcrH_{21–160}$ fragment, which consists of α-helical tetratricopeptide repeats (33, 34). The far-UV CD spectrum of the hisPcrH-PopD complex suggested that PopD also contains a high content of α-helical structure (Fig. 2A, 33). The band with minimum at 208 nm had a larger intensity than the one at 222 nm, suggesting the presence of other secondary structural elements in this complex (35). The far-UV CD spectrum of the hisPcrH-PopB complex was similar to that of hisPcrH-PopD, but the intensity of the bands was lower, suggesting that PopB has less α-helical content than PopD when bound to the PcrH chaperone.

Additionally, we evaluated the local environment around the aromatic residues of the *P. aeruginosa* PAO1 purified proteins. The hisPcrH chaperone contains one Trp and nine Tyr residues, while PopD contains two Tyr and two Trp, and PopB contains one Tyr and one Trp. The emission fluorescence spectra of hisPcrH showed a peak with a maximum at 349 nm (Fig. 2B), indicating that the Trp residue was located in a polar environment, in agreement with the position observed in the X-ray solved structure (34). The shoulder around 303 nm corresponded to the emission of the multiple Tyr residues. The hisPcrH-PopD complex presented an emission fluorescence spectrum similar to hisPcrH, with a maximum at 351 nm. This red-shifted maximum suggested that both the central and C-terminal Trp of PopD reside in a polar environment. In contrast, the emission fluorescence spectrum of hisPcrH-PopB complex showed a maximum at 337 nm, suggesting that the Trp residue of PopB was located in a non-polar environment (Fig. 2B).

The pore formation activity for both purified proteins was analyzed using the florescent assay previously described by us (22). In this assay, a fluorescent marker was encapsulated into liposomes and a quencher was added to the external buffer solution. A high fluorescence intensity signal indicated that the membrane was intact, and the quencher could not contact the fluorophore. If a transmembrane pore is formed upon addition of protein, the fluorophore becomes accessible to the quencher and the fluorescent signal decreases. Both PopB and PopD dissociate from PcrH *in vitro* when the solution pH drops to 5.3, forming heterogeneous protein aggregates (15). These dissociated protein aggregates form pores in model membrane systems (16), however, the translocators are presumably secreted as monomers *in vivo* and in the proximity of the target membrane. Under these circumstances binding to the membrane can precede any protein-protein association. We therefore reasoned that the dissociation of the translocators from the chaperone in the presence of liposomes would more accurately represent *in vivo* conditions.

When separated from PcrH by dropping the pH from 8.0 to 5.1 in the presence of lipid membranes, PopB, PopD, and the equimolar mixture of these proteins were able to form pores (Fig. S3A). Interestingly, in contrast with the results observed when protein aggregates were used, no synergy was observed between PopB and PopD (16). It is therefore clear that the history (i.e., aggregation) of the proteins may affect the mechanism by which the translocators form a pore. Since the sequence of the events that leads to the assembly of a membrane-inserted translocon is far from understood, an experimental procedure that replicates the *in vivo* scenario encountered by the proteins after being secreted through the T3S needle is desirable.

An efficient procedure to isolate PopB and PopD derivatives

Insights into the mechanism of protein insertion into lipid bilayers and the interaction of proteins with membranes can be obtained by fluorescence spectroscopy and site-directed fluorescence labeling (36). A Cys residue is introduced by site-directed mutagenesis at a single site in the protein, and the unique Cys is specifically labeled with the fluorophore of choice. Protein-membrane association and protein-protein interactions can be therefore study using FRET, excitation energy migration (homo-FRET), or fluorescence quenching (37–39).

P. aeruginosa PAO1 translocators do not contain Cys residues, and therefore they are optimal substrates for site-directed fluorescent labeling. However, the labeling of isolated translocators in solution is hampered by their intrinsic tendency to aggregate. Introduced Cys residues can be alternatively labeled while the translocator is still bound to the chaperone PcrH. We noticed that in the recently solved x-ray structure of PcrH the three Cys residues are not exposed to the solvent, (34), and therefore we reasoned that the specific labeling of the translocators may be possible even in the presence of the chaperone. However, our initial labeling reactions demonstrated that the chaperone was also efficiently labeled with thiol-specific probes (not shown).

Analysis of the solvent exposure for the native hisPcrH Cys revealed that on average, 2.20 ± 0.03 Cys residues reacted with the Ellman's reagent (DTNB). Interestingly, incubation of hisPcrH with 6 M guanidinium chloride at 37 °C for 1 hr did not increase the reactivity of the hisPcrH Cys residues to DTNB, suggesting that a portion of those residues were forming intra- or inter-molecular disulfide bonds. SEC analysis of purified hisPcrH samples revealed a first small peak eluted at 14.3 mL and a large second peak eluted at 15.3 mL (Fig. S4A). Non-reducing SDS-PAGE analysis of the two peaks revealed that hisPcrH formed intermolecular disulfide bonds in solution (Fig. S4B). Hence, it is clear from these data that the structure of PcrH in solution is dynamic, and the side chains of the amino acids surrounding the Cys residues move and expose the sulfhydryl groups to the solvent (see below).

Any attempts to replace all three Cys residues in PcrH with non-reactive residues (Ala or Ser) rendered a chaperone that can no longer bind PopD (not shown). Therefore, the interpretation of the fluorescence signal and observed spectral changes derived from the single fluorescently labeled translocators would be veiled by the presence of labeled chaperone. The spectroscopic characterization of the translocon assembly mechanism, therefore, requires an efficient separation of the labeled translocators from the labeled hisPcrH chaperone prior to the analysis.

We took advantage of the polyHis tag located at the N-terminus of the chaperone to isolate labeled translocators. After labeling, the translocators were separated from hisPcrH by binding of the hisPcrH-PopD (or hisPcrH-PopB) complex to an IMAC column and a subsequent elution of PopD (or PopB) with buffer containing urea 6 M. Urea did dissociate

PopD or PopB from their cognate chaperone without affecting the interaction of hisPcrH with the IMAC column (Fig. 1D, lanes 4 and 5). Therefore, the single Cys translocator mutants can be labeled while still bound to hisPcrH, and separated from the chaperone in a subsequent step. This is a simple and efficient procedure to obtain the translocator derivatives required for the structural and functional characterization of the T3S translocon (e.g., single fluorescently-labeled translocators).

Spectroscopic and functional characterization of urea-isolated PopB and PopD

We analyzed the structural and functional properties of the urea-isolated translocators using mass spectrometry, far-UV CD, intrinsic protein fluorescence, and pore formation assays using model membranes. The molecular mass of urea-isolated PopB and PopD was determined using ESI-Ion trap mass spectrometry as detailed under experimental procedures. Only one species was detected for each protein sample with a molecular mass of 40,058 Da for PopB (expected value 40,061 Da), and 31,308 Da for PopD (expected value 31,309 Da).

The polarity around the Trp residues for the urea-isolated PopD and PopB was similar to the polarity observed for the proteins complexed with the hisPcrH chaperone (Fig. 2D). PopD and PopB in urea presented a fluorescence emission maximum at 358 nm and 334 nm, respectively. The far-UV CD negative band at 222 nm observed for PopB in urea 6 M suggested that PopB conserved a high proportion of its α-helical structure even in the presence of the chaotropic agent (Fig. 2C). However, the far-UV CD spectrum of PopD in urea 6 M revealed that a sizeable portion of the secondary structure of this translocator was lost in the presence of the chaotropic agent.

Despite the differences observed in their secondary structure, both urea-isolated PopB and PopD conserved their pore forming abilities at a mildly acidic pH (Fig. S3B). The pore formation activity profiles of urea-isolated translocators were very similar to the ones observed when the translocators were directly dissociated from the chaperone by reducing the pH of the medium (Fig. S3). All together, our data indicated that the purification procedure described above constitutes a simple and efficient alternative to obtain highly pure and active PopD, PopB, their mutant derivatives.

Optimization of a model system to analyze the membrane inserted state of the translocators

Unambiguous interpretation of structural data requires that the components under investigation adopt a uniform conformational state. For the structural analysis of assembled T3S translocons, it is essential that the measured fluorescent signal come from probes located in the same conformation (i.e., membrane-inserted translocons). We therefore optimized our model system to maximize the assembly and insertion of the T3S translocators. Three factors affect the assembly of active transmembrane pores in our experimental system: i) the pH of the medium, ii) the presence of negatively charged phospholipids, and iii) the cholesterol concentration of the target membrane.

In membranes containing a mixture of the lipids commonly present in mammalian plasma membranes (i.e., POPC, POPE, POPS and sphingomyelin) and 15 mol% cholesterol, maximal activity for PopB (~60 %) was observed at pH 5.1 or below (Fig. 3A). For PopD, the maximal activity (~90%) was observed below pH 5. Interestingly, the activity of PopD was lower than the activity of PopB above pH 5.1, but it surpassed that observed for PopB at pH values below 4.8, suggesting that the insertion of PopD into membranes is more dependent on acidic residue protonation than the insertion of PopB.

When maintaining a constant POPC,:POPE,:POPS:sphingomyelin molar ratio in the absence or presence of high cholesterol (45 mol %), the pore forming activity of the translocators was less effective than that observed with 15 mol % cholesterol (not shown). Since the activity of PopD and PopB plateau below pH 4.5 at intermediate cholesterol concentrations, we selected pH 4.0–4.3 and 20 mol % cholesterol for our assays to maximize the formation of uniform membrane-inserted translocons.

Negatively charged phospholipids affect the degree of insertion of T3S translocators (15, 16). We therefore analyzed the effect of POPS on the activity of urea-isolated PopB and PopD in membranes containing POPC and a fixed amount of cholesterol (20 mol %). Addition of 15 mol % POPS increased the activity of PopB twofold, and more than three-fold the activity of PopD (Fig. 3B). Doubling the amount of POPS to 30 mol % was not as effective as the addition of only 15 mol % POPS. Thus, to maximize the conformational homogeneity of membrane-inserted translocators and to minimize any effect caused by the variability of the lipid composition of the system, we chose the simplest membrane model system that maximized the formation of transmembrane pores: POPC:POPS:cholesterol at a molar ratio of 65:15:20.

The pore forming activity of urea-isolated PopD, PopB, and a 1:1 mixture of the translocators was studied using this model system. Maximal activity for PopB and PopD was observed below pH 4.8 and pH 4.3, respectively (Fig. 4A). Interestingly, no additive or synergic effect was detected at higher pH, where the individual proteins showed intermediate pore forming activity. Maximal pore formation using these experimental conditions was observed when the protein:lipid ratio was ~1:3000 (Fig. 4B).

High translocator-lipid ratios produced liposome aggregation

Our initial attempts to visualize the membrane inserted PopD using transmission electron microscopy and uranyl acetate 2% as a contrast agent revealed that even when used at 1:1000 protein:lipid ratio, PopD disrupted the liposomes forming tubular membrane structures (not shown). We therefore analyzed the aggregated state of the liposomes using DLS. Isolated liposomes, incubated at pH 4.0, showed a single particle size distribution with an average of 78 nm (expected ~100 nm, see Fig. S7). However, the incubation of the same liposomes with PopD, PopB, or an equimolar mixture of both translocators, using a 1:1000 protein:lipid molar ratio, shifted the average size distribution to 264 nm, 342 nm, and 164 nm, respectively. These data suggested that at this protein:lipid ratio the translocators caused aggregation of the vesicles, specially when added individually. Little or no aggregation was observed when lower protein lipid ratios were used (Fig. S7) Therefore, when performing structural studies in model systems, it is important to confirm that the size of the vesicles is not altered by the addition of the proteins. If aggregation occurs, the structure adopted by the proteins when bound to membranes may differ from the structure adopted when forming discrete transmembrane pores.

We used cryo-EM to directly visualize the liposomes before and after incubation with the translocators, and to determine the optimal protein:lipid ratio to be used in our studies. Surprisingly, extruded liposomes prepared with POPC:POPS:cholesterol at a molar ratio of 65:15:20 were mostly multi-lamellar (Fig. 4C). Using different protein:lipid ratios, we found that addition of an equimolar mixture of both proteins at a protein:lipid ratio at or below 1:3300 did not alter the liposomal structure (Fig. 4C and Fig. S7). Higher protein concentrations (e.g., 1:330), caused liposome aggregation (Fig. 4D and Fig. S7), but no tubular structures were observed by cryo-EM.

PopB and PopD form discrete and stable membrane pores

We analyzed the ability of the urea-isolated translocators to form discrete and stable pores in liposomes encapsulating the streptavidin-Bodipy fluorescent marker (~5 nm diameter). In contrast to fluorescein (Fl) and Fl derivatives (e.g., calcein and Oregon green), the fluorescent properties of the Bodipy dye are stable at acidic pH (40). Binding of biocytin (biotin moiety covalently attached to the amino acid Lys, ~1 nm in diameter) or biotin attached to the protein β-amylase (~ 4 nm in diameter) to streptavidin-Bodipy (~5 nm in diameter for the monomer) produces a two- or three-fold enhancement in the fluorescence intensity of the streptavidin-Bodipy marker (not shown, 41, 42). When the biotin-labeled molecules were externally added to the sample containing intact liposomes, no fluorescence change was detected on the encapsulated streptavidin-Bodipy. Neither biocytin nor proteins like β-amylase or streptavidin-Bodipy can pass through the membrane unless a pore is formed. The size of the pore will dictate which molecules can cross the membrane. Addition of the translocators produced a fluorescence intensity increase only for the samples containing biocytin, and not for the ones containing biotin-β-amylase. These results indicated that the transmembrane pores formed by PopB and PopD were larger than 1 nm in diameter, but not large enough to allow the passage of the β-amylase protein or the encapsulated streptavidin-Bodipy (Fig. 5A).

The stability of the formed pores was determined by adding the enhancer (biocytin) before or after the addition of the translocators. If the pores are stable, the enhancement of the fluorescence intensity of streptavidin-Bodipy will be observed when biocytin is added before or after the incubation with the translocators. In contrast, if the formed pores are not stable and close, the fluorescence will increase only when biocytin is present before the addition of the translocators, and not when added after the incubation. Since the fluorescence intensity increased in both cases (Fig. 5B), it is clear that the formed pores remained stably open for at least 1 hr in this model system. Control experiments without translocators did not show significant fluorescence change.

PopB and PopD binding to membranes also required acidic pH

To precisely determine the binding of the translocators to the target membrane we introduced single Cys residues in PopB at a location close to a predicted TM segment (S164), and in PopD at a location that was found to be exposed to the aqueous solvent in the membrane bound complex (F223, M. Buckner unpublished results). The Cys residues were labeled with Bodipy. As mentioned above, the emission properties of Bodipy are not sensitive to the polarity of the environment and are not affected by pH in the range used in this work (40). Bodipy labeled translocators were isolated from the hisPcrH chaperone by elution with urea 6 M as described for the wild-type proteins (Fig. 1). Pore forming activity of the Bodipy-labeled translocators was similar to the activity of the wild-type proteins.

We first analyzed the binding of the translocators by using FRET. FRET is an effective method for identifying protein-membrane binding under equilibrium conditions (e.g., 37, 43, 44–46). A typical FRET membrane binding experiment requires two fluorescent dyes, a donor (D) located at a specific site in the protein and an acceptor (A) distributed on the surface of the membrane. The Bodipy dye covalently attached to $PopB^{S164C}$ (or $PopD^{F223C}$) was used as the D dye in our FRET experiments, while Rh-PE incorporated into the membrane was the A dye. After excitation by the absorption of a photon, Bodipy can transfer its excited-state energy to Rh-PE. The efficiency of this transfer depends on, among other things, the extent of overlap of the D emission and the A absorption spectra, the relative orientation of the transition dipoles of the D and the A, and more importantly, the distance between the D and the A dyes. The distance at which the efficiency of FRET from the D to the A is 50% is designated R_0 (the R_0 is ~52 Å for the Bodipy/Rh-PE pair, 44).

Since the FRET efficiency is strongly dependent upon the actual distance separating D and A, FRET will be detected if the dyes are within 95 Å of each other, and it will be maximal when the dyes are separated by less than 24 Å. While considerable FRET efficiency is expected for Bodipy dyes close to the membrane surface (i.e., membrane-bound translocators), no significant FRET is expected for unbound proteins since they will reside more than 100 Å away from the membrane surface. FRET efficiency was estimated using the amplitude weighted average lifetime of the D in the presence ($<\tau_{DA}>_a$) or the absence ($<\tau_D>_a$) of the A. The use of lifetime determinations over steady state measurements is advantageous because it minimize the problems associated with the quantification of the D in the presence and absence of the A(30). Two exponential components were used to fit the lifetime data (Fig. S8 and Table 1S). The use of additional exponential components or lifetime distributions in the analysis did not improve data fit. Binding of the translocators was strongly dependent on the pH of the media (Romano et al, manuscript in preparation). We report here the FRET efficiency at binding saturation (pH 4) and at a point of low binding (pH 6). PopB FRET efficiency was 40% lower at pH 6.0 than at pH 4.0, while PopD FRET efficiency was more than 80% lower at pH 6.0 than at pH 4.0 (Fig. 6).

The pH dependent binding of the translocators was independently assessed by separation of the bound and unbound proteins fractions using a sucrose step gradient and ultracentrifugation as described under Experimental Procedures (15, 23, 47). Given the different densities of proteoliposomes and unbound proteins, proteoliposomes containing the bound protein floats to the top of the sucrose cushion while unbound protein remains at the bottom (23). Bodipy-labeled translocators were individually incubated with membranes at the pH of maximal pore formation activity (pH 4.0, see Fig. 4), and at pH 6.0, where the pore forming activity for PopB was significantly lower, and almost null for PopD. The amount of protein isolated in the top fraction (i.e., membrane bound translocator) was quantified using SDS-PAGE followed by fluorescence scanning with a phosphorimager, and reported as the fraction of the total protein bound to membranes (Fig. 6). At pH 4.0, more than 70 % of the added $PopB^{S164C\text{-}Bodipy}$ and more than 90 % of the added $PopD^{F223C\text{-}Bodipy}$ were isolated in the fraction containing the membranes. In contrast, membrane binding at pH 6.0 was only 40 % and 25 % for PopB and PopD, respectively. These data were consistent with the amount of protein binding observed by FRET. Therefore, we concluded from these complementary and independent approaches that the binding of PopB and PopD to the membrane was higher at the pH of maximal activity, and decreased when the pH was closer to neutral.

PopB interacts with PopD on model membranes

We have shown that PopD and PopB have different optimal pH and lipid composition requirements to form pores in membranes (Fig. 3 and 4). Surprisingly, the pore forming properties of the translocators when added together were similar to the ones observed for PopB alone. No synergic effect between PopB and PopD was observed under our experimental conditions (see discussion below). Do the translocators interact with each other at all? We took advantage of the fluorescence properties of Bodipy to determine PopB-PopD association on membranes.

Bodipy dyes change their fluorescence properties significantly when brought into close proximity with one another. At distances of orbital-orbital contact the emission intensity and lifetime of the sample decreases significantly, presumably by the formation of non-fluorescent Bodipy dimers (48). Proximity of Bodipy dyes at longer distances (i.e., between ~20–85 Å) is detected by the decrease in the anisotropy of the sample (depolarization) caused by energy migration (48, 49). Protein-protein association can be in principle determined by changes in the above mentioned fluorescence properties of the sample when Bodipy-labeled proteins are employed (50). We used a Bodipy-labeled PFO derivative (see

supporting information) as a control for how protein-protein association on membranes affects the fluorescence properties of Bodipy. PFO is well characterized cholesterol-dependent cytolysin that forms oligomeric complexes on lipid membranes (51). These complexes are formed by association of up to 50 monomers in a circular ring-like oligomer on the membrane surface. The rings are ~300 Å in diameter (52, 53). We compared a membrane assembled sample containing 100% labeled PFO, where the effects on the fluorescence properties will be maximal, with a sample containing only 10 mol % of the labeled protein (i.e., only 5 of 50 monomers will be labeled on average in each oligomeric complex). The diluted sample showed a 4.5 fold increase in the emission intensity and more than a two fold increase in the amplitude averaged fluorescence lifetime (Table I), showing that addition of unlabeled PFO separated the PFO^{Bodipy} molecules apart, increasing the distance between probes (48). The increase on the distance between probes, caused by the intercalation of unlabeled proteins, also diminished the depolarization of the sample emission caused by Bodipy-Bodipy energy migration (i.e., the anisotropy increased, Table I, 54).

We assessed the interaction between PopB and PopD using $PopD^{Bodipy}$ and analyzed the changes in the fluorescence properties of the sample when the labeled translocator was mixed with unlabeled PopB (and vice versa). As expected for the formation of mixed protein complexes containing both PopB and PopD in the membrane, dilution of $PopD^{Bodipy}$ with unlabeled PopB increased the emission intensity and the amplitude averaged fluorescence lifetime of Bodipy (Table 1). When compared to the data obtained for the PFO oligomer, it is clear that unlabeled PopB intercalated between labeled PopD proteins when bound to the membrane. The significant but relatively smaller increase on the anisotropy for Bodipy labeled translocators suggested that PopD and PopB formed heteromeric complexes with smaller size than the large ~300 Å diameter rings formed by PFO, as Bodipy-Bodipy energy migration only occurs at distances shorter than 100 Å. Similar changes were detected when $PopB^{Bodipy}$ was diluted with unlabeled PopD. The smaller changes in the fluorescence parameters observed for $PopB^{Bodipy}$ reflected the lower percentage of labeling of this derivative (68% vs 96% for $PopD^{Bodipy}$). Thus, we conclude that when added together, PopB associated with PopD to assemble pore-forming complexes on model membranes.

DISCUSSION

Structural and functional characterization of the T3S translocators is inherently difficult given the non-polar nature of the proteins and their tendency to aggregate in solution. Co-expression of T3S recombinant translocators in the presence of their cognate chaperone renders soluble protein complexes and allows their purification in large quantities (15, 31–33). However, the analysis of individual T3S translocators requires their separation from the chaperone prior to their assembly into membranes. These separations have been achieved by reducing the pH of the medium (15, 31) or by the inclusion of mild detergents (31). Unfortunately, upon dissociation from the PcrH chaperone, both PopB and PopD form large and non-uniform protein aggregates (15) that make it difficult to characterize the protein-membrane and protein-protein association processes. Furthermore, we observed that during the acidification of the medium to separate the translocators from the chaperone, PcrH precipitates carrying considerable amounts of the purified translocators (Fig. S5). Thus, the precise characterization of the T3S translocon assembly into membranes required a more efficient experimental approach to isolate active translocators.

We have found in these studies that PopB (as well as PopD) can be purified as a homogeneous complex with the cognate chaperone hisPcrH and be effectively dissociated and isolated from hisPcrH using urea. In contrast to PopD, which lost most of its secondary structure, PopB retained a high proportion of its secondary structure after solubilization in

urea 6 M. The blue-shifted intrinsic fluorescence spectra of urea solubilized PopB, suggested that the Trp located at the N-terminus of a predicted TM segment (residues 169–187) remained located in a non-polar environment even in the denatured state. As expected for proteins that are proposed to travel unfolded through the T3S needle and to be released in close proximity of the target membrane, both urea-isolated translocators formed discrete and stable TM pores upon dilution in the presence of lipid bilayers. The pore forming properties of urea-isolated PopB and PopD were consistent with the ones described previously for translocators isolated using low pH (16). Interestingly, quantitative assessment of PopB and PopD binding to membranes showed that acidic pH was not only required for membrane insertion, but also for a stable protein-membrane interaction. In summary, we have established an efficient experimental procedure to isolate native and modified forms of PopB and PopD, and to specifically label the translocators with fluorescent or other type of probes (e.g., cross-linkers). Isolated translocators were assembled on model membranes where they form discrete and stable pores. Moreover, our spectroscopic examination of Bodipy-labeled translocators showed that when added together, PopB intercalates with PopD on membrane assembled complexes.

Purification of isolated recombinant translocators has shown to be a difficult task. PopD cloned in pET based vector systems produced large amounts of protein, but mostly as inclusion bodies. The yield of water-soluble PopD can be improved by expression at low temperature (i.e., ~18°C), but water-soluble PopD forms aggregates (15, *and data not shown*). PopB is toxic for *Escherichia coli* cells and cannot be stably produced (data not shown). Schoehn et al (15) elegantly solved these problems by co-expressing the translocators with their cognate chaperone PcrH. The water-soluble PcrH-PopD 1:1 complex was obtained in large amounts and the structural characterization of PopD showed it adopts a molten globular conformation (33). Less is known about the structure of PopB, given that only minor amounts of a homogeneous PcrH-PopB complex were obtained using this procedure (15, 32).

We found that the purified hisPcrH-PopB complex can remain soluble and non-aggregated in aqueous solutions at relative low concentrations (Fig. 1 and S1). The structure of purified hisPcrH-PopB complex was analyzed using a combination of CD and fluorescence spectroscopy (Fig. 2). Far-UV CD analysis revealed that PopB had less α-helical content than PopD when bound to hisPcrH. However, in contrast to the low secondary structure content observed in urea-isolated PopD, urea-isolated PopB retained considerable amount of secondary structure. Furthermore, the only Trp of PopB was located in a non-polar environment when bound to the chaperone or when denatured in urea. These data suggested that PopB adopts a more compact conformation than the one observed for molten globular PopD (33).

PopB and PopD remain stably bound to PcrH in the bacterial cytoplasm in the absence of secretion, most likely to avoid protein aggregation and to maintain a secretion-competent conformation (7, 9). After bacterium contact with the target cell, PopB and PopD dissociate from PcrH and are presumably secreted through a narrow channel formed by the T3S needle (2–2.5 nm in diameter). Unfolded translocators are proposed to emerge from the tip of the T3S needle (formed by PcrV), in close proximity of the target membrane. PcrV is required to engage the membrane inserted translocon with the T3S needle (13, 55, 56) however PcrV is not involved in the formation of the TM pore (15). Therefore, the use of urea-isolated translocators to reconstitute membrane-inserted protein complexes is reasonable since the dilution of urea-isolated PopB and PopD in the presence of membranes likely resembles the *in vivo* translocon assembly process.

While negatively charged phospholipids are crucial for the binding of translocators to membranes and formation of TM pores in model membranes, cholesterol seems not to play a central role *in vitro* (16). We tested how different lipids affected the pore formation properties of PopB and PopD in our experimental system. The presence of cholesterol and POPS in the liposomal membranes facilitated the insertion of the urea-isolated PopB and PopD (Fig. 3). Other lipids like sphingomyelin and PE did not significantly altered the pore formation efficiency observed with liposomes composed of POPC:POPS:cho (65:15:20 molar ratio, data not shown). Therefore, we chose this composition as a simple and efficient model membrane system to study the assembly of PopB and PopD into lipid bilayers. Urea-isolated translocators formed discrete and stable pores in model membranes (Fig. 4 and 5). Taken together, our data showed that the treatment with urea 6 M did not significantly alter the pore formation properties of the translocators.

We found that urea-isolated PopB, PopD, or an equimolar mixture of both translocators formed pores very similar to the pores formed when the translocators are dissociated from PcrH at acidic pH in the presence of membranes (Fig. S3). Interestingly, the comparison of both experimental systems suggested that acidic pH was not only required to dissociate the translocators from the chaperone (Fig. S5), but also to promote binding and insertion of translocators into membranes (Fig. 4 and 6). We employed two independent experimental approaches, time-resolved FRET and sucrose-step gradient ultracentrifugation, to analyze the binding of the translocators to membranes at different pHs (Fig. 6). Both assays clearly showed that binding at pH 4 was more efficient than at pH 6. Only a small fraction of the proteins was found associated with the membranes at pH 6. These results differ from the ones previously observed when heterogeneous aggregates of PopB and PopD were used (16). The kinetics parameters used as a measure of membrane binding may represent the behavior of a small fraction of protein in the experimental system, and not necessarily the average behavior of all the protein in the sample (i.e., unbound protein does not generate a signal). Our data suggested that the decrease in the activity of the translocators at higher pH was, at least in part, caused by the inability of the proteins to bind to the lipid membrane.

A homogeneous sample is essential for the unambiguous interpretation of the spectroscopic signal obtained during the analysis of protein complexes assembled into membranes (39). For this purpose, negatively charged phospholipid and low pH have been extensively used in the spectroscopic studies of pore-forming proteins like colicins, diphtheria toxin, Bcl-x_L, etc. (57–61). The requirement of acidic pH for protein insertion into membranes has been associated with the presence of acidic molten globular states (62). While this pH dependent conformational change may be relevant to the more compact PopB conformation (see above), PopD was found to have a molten globule conformation even at neutral pH (33). Therefore, the spontaneous insertion of PopD (and/or PopB) segments into lipid bilayers may require the protonation of acidic residues, as shown before for bacteriorhodopsin fragments (63). In our model system, the use of acidic pH maximized the assembly of discrete and stable TM pores. Such a low pH is presumably not encountered by the proteins when interacting with the plasma membrane of the target cell *in vivo*. Clearly, other still unidentified components present in the bacterium, or in the target cell, may facilitate the assembly of the translocon but further studies are required in this area.

It has been widely assumed that assembled translocons contain both translocators forming a hetero-oligomer (9). However, the structural arrangement of the membrane-inserted translocon and the stoichiometry of the complex are not known. By combining site directed fluorescence labeling with both excitation energy migration and fluorescence quenching, we have shown that fluorescently-labeled PopB interacted with native PopD in intact membrane-inserted complexes (Table 1). This interaction was confirmed by using the reverse combination of labeled PopD and native PopB. In both experiments, the

intercalation of unlabeled molecules among the labeled ones produced the separation of the Bodipy dyes, and consequently an increase in the fluorescence intensity, lifetime, and anisotropy of the sample. These results also implied that when added individually, both PopD$^{F223C\text{-}Bodipy}$ and PopB$^{S164C\text{-}Bodipy}$ formed homo-oligomers. Self interaction of the translocators in intact membrane-inserted complexes was confirmed by the relative increase of the fluorescence intensity, the lifetimes, and the anisotropy of the sample when native PopD (or PopB) was mixed with PopD $^{F223C\text{-}Bodipy}$ (or PopB $^{S164C\text{-}Bodipy}$) and added to the membranes (data not shown).

In summary, we have established a cell-free system to analyze the structural assembly of the *P. aeruginosa* T3S translocators. Using this system, we found that PopB interacts with PopD when forming discrete and stable pores in intact membranes. Cell-free systems have been extremely useful to examine interactions among relevant protein components in membrane protein complexes and the study of their assembly and their structure (e.g., 44, 46, 57, 61, 64–66) The identified mechanism and structural information obtained using cell-free system are very valuable to design *in vivo* experiments and evaluate the contribution of other known or unknown factors to the mechanism of T3S effector translocation.

Supplementary Material

Refer to Web version on PubMed Central for supplementary material.

Acknowledgments

We thank Prof. Carlos F. Gonzalez (Texas A&M University) for providing the *Pseudomonas aeruginosa* PAO1 genomic DNA, Prof. Lila M. Gierasch for assistance on the CD measurements, Prof. Christopher Woodcock for his assistance on the initial transmission EM experiments, William Boston-Howes for the preliminary set-up of the liposome flotation assay, Michael Buckner for preparation of the PopD^{F223C} mutant, and Sarah E. Kells for excellent technical assistance.

Abbreviations

Pop	*Pseudomonas* outer protein
Pcr	*Pseudomonas* low calcium response
T3S	Type III secretion
TM	transmembrane
IMAC	immobilized metal ion affinity chromatography
AEC	anion exchange chromatography
SEC	size exclusion chromatography
UV	ultraviolet
CD	circular dichroism
DLS	dynamic light scattering
POPC	1-palmitoyl-2-oleoyl-*sn*-glycero-3-phosphocholine
POPE	1-palmitoyl-2-oleoyl-*sn*-glycero-3-phosphoethanolamine
POPS	1-palmitoyl-2-oleoyl-*sn*-glycero-3-phospho-L-serine
Fl	fluorescein
DTT	(*2S*,*3S*)-1,4-bis-sulfanylbutane-2,3-diol

EDTA	ethylenedinitrilotetraacetic acid
DPA	dipicolinic acid
HEPES	2-[4-(2-hydroxyethyl)piperazin-1-yl]ethanesulfonic acid
LB	Luria-Bertani
IPTG	isopropyl α-D-thiogalactopyranoside
Tris	2-Amino-2-hydroxymethyl-propane-1,3-diol
FRET	Förster resonance energy transfer
SDS-PAGE	sodium dodecyl sulfate polyacrylamide gel electrophoresis
Rh-PE	rhodamine B 1,2-dihexadecanoyl-sn-glycero-3-phosphoethanolamine
Bodipy	4,4-difluoro-5,7-dimethyl-4-bora-3a,4a-diaza-3-indacene
PFO	Perfringolysin O

References

1. Hueck CJ. Type III protein secretion systems in bacterial pathogens of animals and plants. Microbiol Mol Biol Rev. 1998; 62:379–433. [PubMed: 9618447]
2. Galan JE, Wolf-Watz H. Protein delivery into eukaryotic cells by type III secretion machines. Nature. 2006; 444:567–573. [PubMed: 17136086]
3. Cornelis GR. The type III secretion injectisome. Nat Rev Micro. 2006; 4:811–825.
4. Frank D. The exoenzyme S regulon of *Pseudomonas aeruginosa*. Mol Microbiol. 1997; 26:621–629. [PubMed: 9427393]
5. Hauser AR, Cobb E, Bodi M, Mariscal D, Valles J, Engel JN, Rello J. Type III protein secretion is associated with poor clinical outcomes in patients with ventilator-associated pneumonia caused by *Pseudomonas aeruginosa*. Crit Care Med. 2002; 30:521–528. [PubMed: 11990909]
6. Moraes TF, Spreter T, Strynadka NCJ. Piecing together the type III injectisome of bacterial pathogens. Curr Op Struct Biol. 2008; 18:258–266.
7. Mueller CA, Broz P, Cornelis GR. The type III secretion system tip complex and translocon. Molec Microbiol. 2008; 68:1085–1095. [PubMed: 18430138]
8. Buttner D, Bonas U. Port of entry - the type III secretion translocon. Trends Microbiol. 2002; 10:186–192. [PubMed: 11912026]
9. Matteï PJ, Faudry E, Job V, Izoré T, Attree I, Dessen A. Membrane targeting and pore formation by the type III secretion system translocon. FEBS J. 2011; 278:414–426. [PubMed: 21182592]
10. Mueller CA, Broz P, Muller SA, Ringler P, Erne-Brand F, Sorg I, Kuhn M, Engel A, Cornelis GR. The V-antigen of *Yersinia* forms a distinct structure at the tip of injectisome needles. Science. 2005; 310:674–676. [PubMed: 16254184]
11. Dacheux D, Goure J, Chabert J, Usson Y, Attree I. Pore-forming activity of type III system-secreted proteins leads to oncosis of *Pseudomonas aeruginosa*-infected macrophages. Mol Microbiol. 2001; 40:76–85. [PubMed: 11298277]
12. Sundin C, Thelaus J, Broms JE, Forsberg A. Polarisation of type III translocation by *Pseudomonas aeruginosa* requires PcrG, PcrV and PopN. Microb Pathog. 2004; 37:313–322. [PubMed: 15619427]
13. Goure J, Pastor A, Faudry E, Chabert J, Dessen A, Attree I. The V antigen of *Pseudomonas aeruginosa* is required for assembly of the functional PopB/PopD translocation pore in host cell membranes. Infect Immun. 2004; 72:4741–4750. [PubMed: 15271936]
14. Vance RE, Rietsch A, Mekalanos JJ. Role of the type III secreted exoenzymes S, T, and Y in systemic spread of *Pseudomonas aeruginosa* PAO1 *in vivo*. Infect Immun. 2005; 73:1706–1713. [PubMed: 15731071]

15. Schoehn G, Di Guilmi AM, Lemaire D, Attree I, Weissenhorn W, Dessen A. Oligomerization of type III secretion proteins PopB and PopD precedes pore formation in *Pseudomonas*. EMBO J. 2003; 22:4957–4967. [PubMed: 14517235]
16. Faudry E, Vernier G, Neumann E, Forge V, Attree I. Synergistic pore formation by type III toxin translocators of *Pseudomonas aeruginosa*. Biochemistry. 2006; 45:8117–8123. [PubMed: 16800636]
17. Tardy F, Homble F, Neyt C, Wattiez R, Cornelis G, Ruysschaert J, Cabiaux V. *Yersinia enterocolitica* type III secretion-translocation system: Channel formation by secreted Yops. EMBO J. 1999; 18:6793–6799. [PubMed: 10581252]
18. Hume PJ, McGhie EJ, Hayward RD, Koronakis V. The purified *Shigella* IpaB and *Salmonella* SipB translocators share biochemical properties and membrane topology. Mol Microbiol. 2003; 49:425–439. [PubMed: 12828640]
19. Pace CN, Vajdos F, Fee L, Grimsley G, Gray T. How to measure and predict the molar absorption coefficient of a protein. Protein Sci. 1995; 4:2411–2423. [PubMed: 8563639]
20. Moe PC, Heuck AP. Phospholipid hydrolysis caused by *Clostridium perfringens* α– toxin facilitates the targeting of perfringolysin O to membrane bilayers. Biochemistry. 2010; 49:9498–9507. [PubMed: 20886855]
21. Shepard LA, Heuck AP, Hamman BD, Rossjohn J, Parker MW, Ryan KR, Johnson AE, Tweten RK. Identification of a membrane-spanning domain of the thiol-activated pore-forming toxin *Clostridium perfringens* perfringolysin O: An alpha-helical to beta-sheet transition identified by fluorescence spectroscopy. Biochemistry. 1998; 37:14563–14574. [PubMed: 9772185]
22. Heuck AP, Tweten RK, Johnson AE. Assembly and topography of the prepore complex in cholesterol-dependent cytolysins. J Biol Chem. 2003; 278:31218–31225. [PubMed: 12777381]
23. Dalton AK, Murray PS, Murray D, Vogt VM. Biochemical characterization of Rous sarcoma virus MA protein interaction with membranes. J Virol. 2005; 79:6227–6238. [PubMed: 15858007]
24. Koppel DE. Analysis of macromolecular polydispersity in intensity correlation spectroscopy: The method of cumulants. J Chem Physs. 1972; 57:4814–4820.
25. Reinhart GD, Marzola P, Jameson DM, Gratton E. A method for online background subtraction in frequency domain fluorometry. J Fluorescence. 1991; 1:153–162.
26. Crowley KS, Liao S, Worrell VE, Reinhart GD, Johnson AE. Secretory proteins move through the endoplasmic reticulum membrane via an aqueous, gated pore. Cell. 1994; 78:461–471. [PubMed: 8062388]
27. vandeVen M, Ameloot M, Valeur B, Boens N. Pitfalls and their remedies in time-resolved fluorescence spectroscopy and microscopy. J Fluorescence. 2005; 15:377–413.
28. Boens N, Qin W, Basaric N, Hofkens J, Ameloot M, Pouget J, Lefevre JP, Valeur B, Gratton E, vandeVen M, Silva ND, Engelborghs Y, Willaert K, Sillen A, Rumbles G, Phillips D, Visser AJWG, vanHoek A, Lakowicz JR, Malak H, Gryczynski I, Szabo AG, Krajcarski DT, Tamai N, Miura A. Fluorescence lifetime standards for time and frequency domain fluorescence spectroscopy. Anal Chem. 2007; 79:2137–2149. [PubMed: 17269654]
29. Alcala JR, Gratton E, Prendergast FG. Resolvability of fluorescence lifetime distributions using phase fluorometry. Biophys J. 1987; 51:587–596. [PubMed: 3580485]
30. Wu PG, Brand L. Resonance energy transfer: Methods and applications. Anal Biochem. 1994; 218:1–13. [PubMed: 8053542]
31. Birket SE, Harrington AT, Espina M, Smith ND, Terry CM, Darboe N, Markham AP, Middaugh CR, Picking WL, Picking WD. Preparation and characterization of translocator/chaperone complexes and their component proteins from *Shigella flexneri*. Biochemistry. 2007; 46:8128–8137. [PubMed: 17571858]
32. Tan YW, Yu HB, Sivaraman J, Leung KY, Mok YK. Mapping of the chaperone AcrH binding regions of translocators AopB and AopD and characterization of oligomeric and metastable AcrH-AopB-AopD complexes in the type III secretion system of *Aeromonas hydrophila*. Prot Scien. 2009; 18:1724–1734.
33. Faudry E, Job V, Dessen A, Attree I, Forge V. Type III secretion system translocator has a molten globule conformation both in its free and chaperone-bound forms. FEBS J. 2007; 274:3601–3610. [PubMed: 17578515]

34. Job V, Matteï P-J, Lemaire D, Attree I, Dessen Aa. Structural basis of chaperone recognition of type III secretion system minor translocator proteins. J Biol Chem. 2010; 285:23224–23232. [PubMed: 20385547]
35. Manavalan P, Johnson WC. Sensitivity of circular dichroism to protein tertiary structure class. Nature. 1983; 305:831–832.
36. Heuck AP, Johnson AE. Pore-forming protein structure analysis in membranes using multiple independent fluorescence techniques. Cell Biochem Biophys. 2002; 36:89–101. [PubMed: 11939373]
37. Mutucumarana VP, Duffy EJ, Lollar P, Johnson AE. The active site of factor IXa is located far above the membrane surface and its conformation is altered upon association with factor VIIIa. A fluorescence study. J Biol Chem. 1992; 267:17012–17021. [PubMed: 1512240]
38. Hamman BD, Oleinikov AV, Jokhadze GG, Traut RR, Jameson DM. Dimer/monomer equilibrium and domain separations of *Escherichia coli* ribosomal protein L7/L12. Biochemistry. 1996; 35:16680–16686. [PubMed: 8988004]
39. Johnson AE. Fluorescence approaches for determining protein conformations, interactions and mechanisms at membranes. Traffic. 2005; 6:1078–1092. [PubMed: 16262720]
40. Karolin J, Johansson LBA, Strandberg L, Ny T. Fluorescence and absorption spectroscopic properties of dipyrrometheneboron difluoride (Bodipy) derivatives in liquids, lipid membranes, and proteins. J Am Chem Soc. 1994; 116:7801–7806.
41. Nicol F, Nir S, Szoka FC Jr. Orientation of the pore-forming peptide gala in POPC vesicles determined by a Bodipy-avidin/biotin binding assay. Biophys J. 1999; 76:2121–2141. [PubMed: 10096907]
42. Rosconi MP, Zhao G, London E. Analyzing topography of membrane-inserted diphtheria toxin T domain using Bodipy-streptavidin: At low pH, helices 8 and 9 form a transmembrane hairpin but helices 5–7 form stable nonclassical inserted segments on the cis side of the bilayer. Biochemistry. 2004; 43:9127–9139. [PubMed: 15248770]
43. Bazzi MD, Nelsestuen GL. Association of protein kinase C with phospholipid vesicles. Biochemistry. 1987; 26:115–122. [PubMed: 3103676]
44. Ramachandran R, Tweten RK, Johnson AE. The domains of a cholesterol-dependent cytolysin undergo a major fret-detected rearrangement during pore formation. Proc Natl Acad Sci USA. 2005; 102:7139–7144. [PubMed: 15878993]
45. Posokhov YO, Ladokhin AS. Lifetime fluorescence method for determining membrane topology of proteins. Anal Biochem. 2006; 348:87–93. [PubMed: 16298322]
46. Lovell JF, Billen LP, Bindner S, Shamas-Din A, Fradin C, Leber B, Andrews DW. Membrane binding by tBid initiates an ordered series of events culminating in membrane permeabilization by Bax. Cell. 2008; 135:1074–1084. [PubMed: 19062087]
47. Rivnay B, Metzger H. Use of the airfuge for analysis and preparation of receptors incorporated into liposomes: Studies with the receptor for immunoglobulin E. Anal Biochem. 1983; 130:514–520. [PubMed: 6223542]
48. Bergstrom F, Mikhalyov I, Hagglof P, Wortmann R, Ny T, Johansson LBA. Dimers of dipyrrometheneboron difluoride (Bodipy) with light spectroscopic applications in chemistry and biology. J Am Chem Soc. 2002; 124:196–204. [PubMed: 11782171]
49. Mikhalyov, l; Gretskaya, N.; Bergström, F.; Johansson, LB-Å. Electronic ground and excited state properties of dipyrrometheneboron difluoride (Bodipy): Dimers with application to biosciences. Phys Chem Chem Phys. 2002; 4:5663–5670.
50. Marushchak D, Kalinin S, Mikhalyov I, Gretskaya N, Johansson LB-Å. Pyrromethene dyes (Bodipy) can form ground state homo and hetero dimers: Photophysics and spectral properties. Spectrochim Acta Part A. 2006; 65:113–122.
51. Heuck, AP.; Moe, PC.; Johnson, BB. The cholesterol-dependent cytolysins family of Gram-positive bacterial toxins. In: Harris, JR., editor. Cholesterol binding proteins and cholesterol transport. Springer; 2010. p. 551-577.
52. Czajkowsky DM, Hotze EM, Shao Z, Tweten RK. Vertical collapse of a cytolysin prepore moves its transmembrane beta-hairpins to the membrane. EMBO J. 2004; 23:3206–3215. [PubMed: 15297878]

53. Dang TX, Hotze EM, Rouiller I, Tweten RK, Wilson-Kubalek EM. Prepore to pore transition of a cholesterol-dependent cytolysin visualized by electron microscopy. J Struct Biol. 2005; 150:100–108. [PubMed: 15797734]
54. Jameson DM, Croney JC, Moens PDJ, Gerard Marriott, Ian P. Fluorescence: Basic concepts, practical aspects, and some anecdotes. Meth Enzymol. 2003; 360:1–43. [PubMed: 12622145]
55. Sawa T, Yahr TL, Ohara M, Kurahashi K, Gropper MA, Wiener-Kronish JP, Frank DW. Active and passive immunization with the *Pseudomonas* V antigen protects against type III intoxication and lung injury. Nat Med. 1999; 5:392–398. [PubMed: 10202927]
56. Goure J, Broz P, Attree O, Cornelis GR, Attree I. Protective anti-V antibodies inhibit *Pseudomonas* and *Yersinia* translocon assembly within host membranes. J Infect Dis. 2005; 192:218–225. [PubMed: 15962216]
57. Wang Y, Malenbaum SE, Kachel K, Zhan H, Collier RJ, London E. Identification of shallow and deep membrane-penetrating forms of diphtheria toxin T domain that are regulated by protein concentration and bilayer width. J Biol Chem. 1997; 272:25091–25098. [PubMed: 9312118]
58. Chenal A, Savarin P, Nizard P, Guillain F, Gillet D, Forge V. Membrane protein insertion regulated by bringing electrostatic and hydrophobic interactions into play. A case study with the translocation domain of the diphtheria toxin. J Biol Chem. 2002; 277:43425–43432. [PubMed: 12193591]
59. Thuduppathy GR, Terrones O, Craig JW, Basanez G, Hill RB. The N-terminal domain of Bcl-x_l reversibly binds membranes in a pH-dependent manner. Biochemistry. 2006; 45:14533–14542. [PubMed: 17128992]
60. Musse AA, Wang J, deLeon GP, Prentice GA, London E, Merrill AR. Scanning the membrane-bound conformation of helix 1 in the colicin E1 channel domain by site-directed fluorescence labeling. J Biol Chem. 2006; 281:885–895. [PubMed: 16299381]
61. Kyrychenko A, Posokhov YO, Rodnin MV, Ladokhin AS. Kinetic intermediate reveals staggered pH-dependent transitions along the membrane insertion pathway of the diphtheria toxin T-domain. Biochemistry. 2009; 48:7584–7594. [PubMed: 19588969]
62. van der Goot FG, Gonzalez-Manas JM, Lakey JH, Pattus F. A 'molten-globule' membrane-insertion intermediate of the pore-forming domain of colicin A. Nature. 1991; 354:408–410. [PubMed: 1956406]
63. Hunt JF, Rath P, Rothschild KJ, Engelman DM. Spontaneous, pH-dependent membrane insertion of a transbilayer alpha-helix. Biochemistry. 1997; 36:15177–15192. [PubMed: 9398245]
64. Shatursky O, Heuck AP, Shepard LA, Rossjohn J, Parker MW, Johnson AE, Tweten RK. The mechanism of membrane insertion for a cholesterol-dependent cytolysin: A novel paradigm for pore-forming toxins. Cell. 1999; 99:293–299. [PubMed: 10555145]
65. Musse AA, Merrill AR. The molecular basis for the pH-activation mechanism in the channel-forming bacterial colicin E1. J Biol Chem. 2003; 278:24491–24499. [PubMed: 12714593]
66. Zakharov SD, Sharma O, Zhalnina MV, Cramer WA. Primary events in the colicin translocon: FRET analysis of colicin unfolding initiated by binding to BtuB and OmpF. Biochemistry. 2008; 47:12802–12809. [PubMed: 18986168]

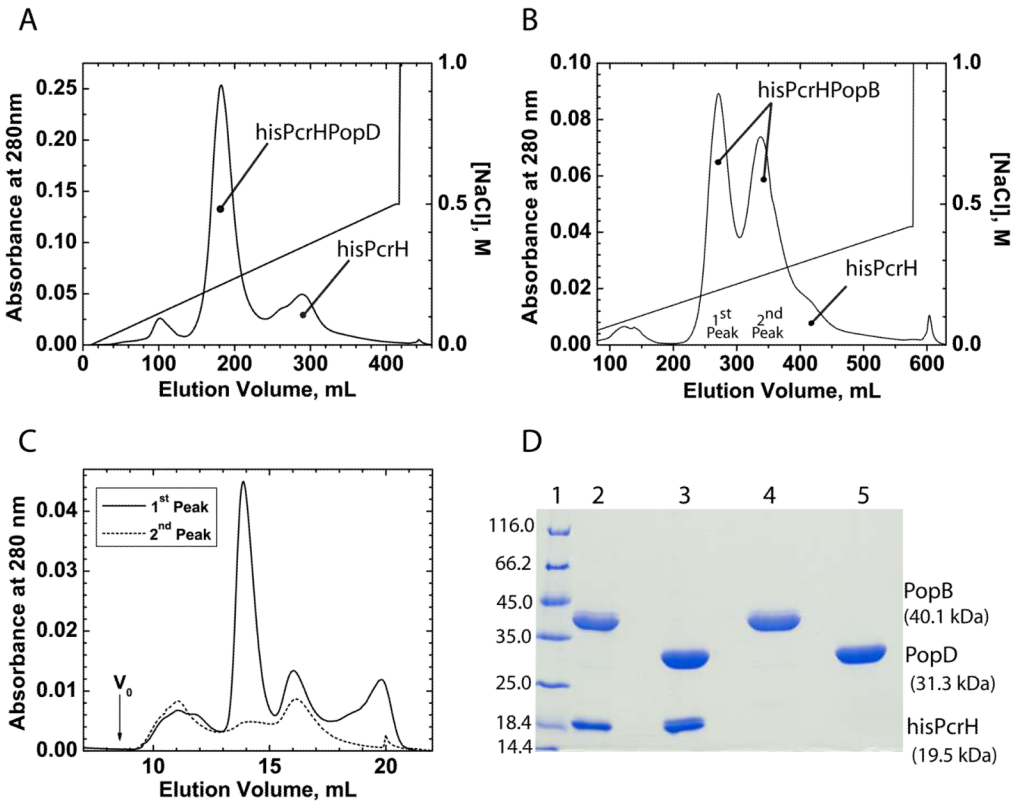

Figure 1. Purification of the hisPcrH-translocator complexes

(A) The fractions containing the hisPcrH-PopD complex isolated after the first IMAC purification step were dialyzed and loaded into a Q-Sepharose AEC column and eluted using a linear NaCl gradient. The peaks containing hisPcrH and hisPcrH-PopD are indicated. (B) The hisPcrH-PopB complex was purified as described for hisPcrH-PopD. The first two large peaks that eluted from the AEC contained the hisPcrH-PopB complexes and the shoulder that eluted around 400 mL contained hisPcrH. (C) SEC analysis of aliquots corresponding to the 1st Peak and the 2nd Peak illustrated in B. (D) SDS-PAGE analysis of purified proteins. Lane 1, molecular weight markers; lane 2, hisPcrH-PopB; lane 3, hisPcrH-PopD; lanes 4 and 5, urea-isolated PopB and PopD, respectively.

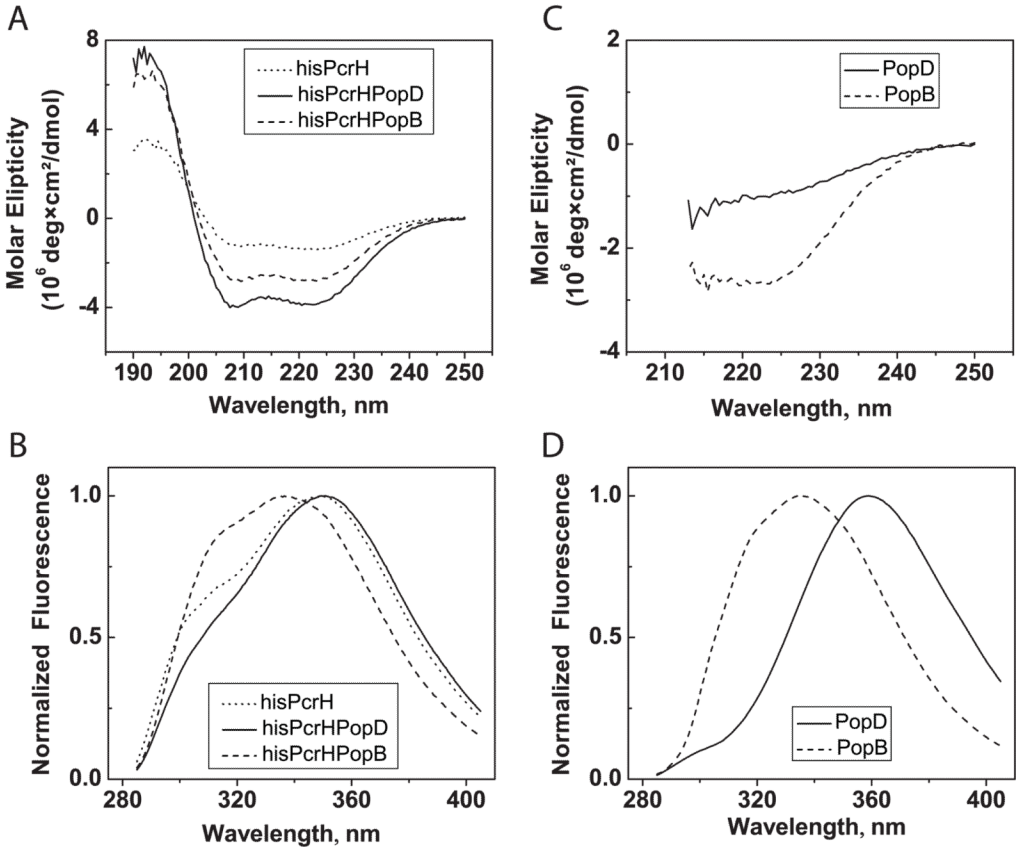

Figure 2. Characterization of purified translocators

(A) Far UV CD spectra of the SEC-isolated hisPcrH, hisPcrH-PopD, and hisPcrH-PopB recorded in buffer E, total protein concentration was 3.0 μM. (B) Normalized fluorescence emission spectra of hisPcrH, hisPcrH-PopD, and hisPcrH-PopB recorded in buffer E. Excitation wavelength was 278 nm, total protein concentration was 2.4 μM. (C) Far UV CD spectra of purified PopD and PopB recorded in phosphate buffer 20 mM, pH 7.5 supplemented with urea 6 M, protein concentration was 2.4 μM. (D) Normalized fluorescence emission spectra of PopD and PopB in phosphate buffer 20 mM, pH 7.5 supplemented with urea 6 M. Excitation wavelength was 278 nm, total protein concentration was 2.4 μM.

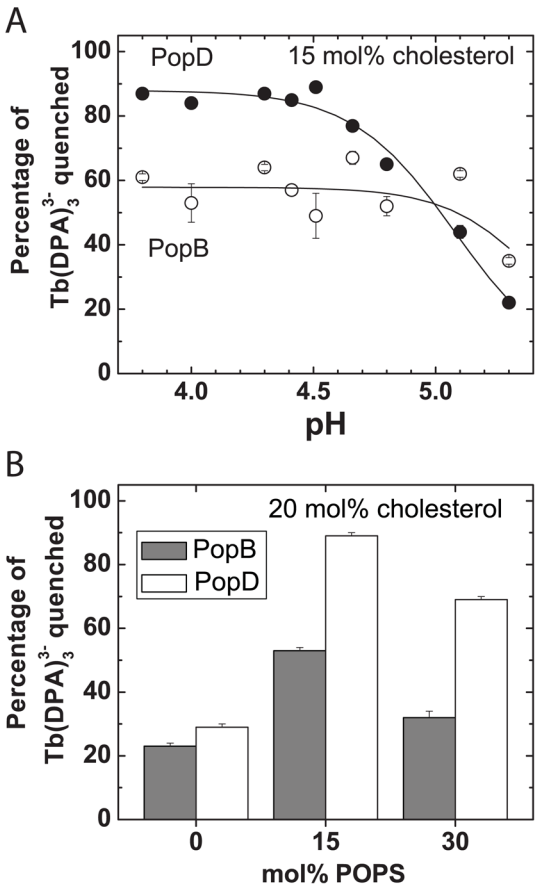

Figure 3. Effect of pH and lipid composition on the pore forming activity of the urea-isolated translocators

Pore formation was determined as the percentage of the encapsulated $Tb(DPA)_3^{3-}$ that was quenched by EDTA as detailed in experimental procedures. (A) Urea-isolated PopB or PopD were directly diluted into a solution of 50 mM sodium acetate buffered at the indicated pH, containing membranes. The pore forming activity of the urea-isolated translocators increased at acidic pH. The total lipid concentration was 0.1 mM and the liposomes composition was 35 mol % POPC, 18 mol % POPS, 24 mol % POPE, 17 mol% SM, and 15 mol % cholesterol. Protein:lipid ratio was 1:1000. (B) Effect of POPS on the pore formation activity of urea-isolated translocators. The activity was measured as described in A, the pH was buffered at 4.3, and the lipid composition was POPC, 20 mol % cholesterol, and the indicated concentration of POPS.

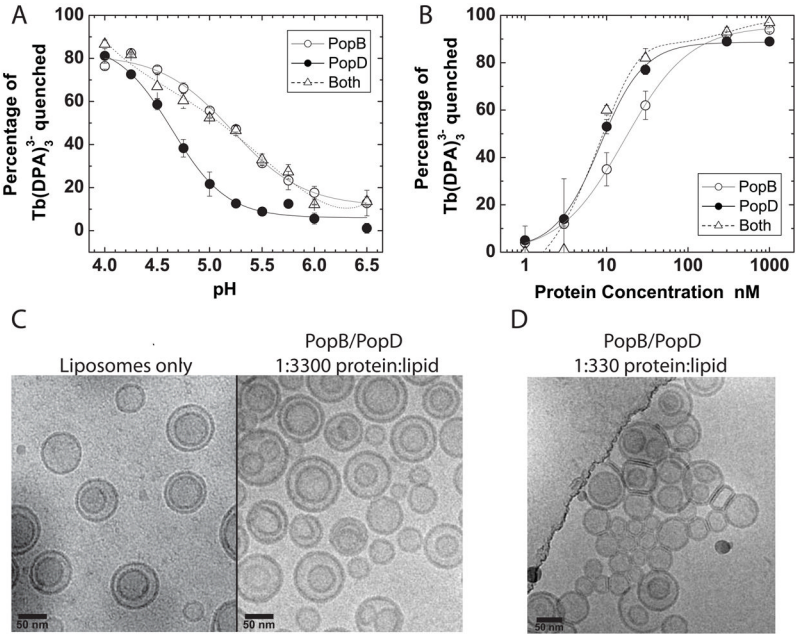

Figure 4. Pore forming activity of the urea-isolated translocators

Pore formation was determined as the percentage of the encapsulated $Tb(DPA)_3^{3-}$ that was quenched by EDTA as detailed in experimental procedures. (A) Urea-isolated PopB, PopD, or an equimolar mixture of both proteins were diluted into a buffer solution containing membranes at the indicated pH. Total concentration of lipids was 0.15 mM. Total protein concentration was 60 nM for the PopB and PopD traces (protein:lipid ratio 1/2500), and 120 nM when PopB and PopD where added together (protein:lipid ratio 1/1250). (B) Concentration-dependent pore formation by PopD, PopB (protein:lipid ratio ranged from $1/10^5$ to 1/100), or an equimolar mixture of both proteins diluted into buffer D containing 0.1 mM total lipids. When both proteins were added together the sample contained twice as much total protein than the concentration indicated in the graph (protein:lipid ratio ranged from $1/5.10^4$ to 1/50). (C) Cryo-electron micrographs of liposomes with and without PopB/PopD at the indicated protein:lipid ratios. Buffer B was added to the control sample with only liposomes to assess any effect in membrane structure due to residual urea concentration. Lipid concentration was 5 mM in all cases and total protein concentration was 1.5 μM or 15 μM. The POPC:cholesterol:POPS molar ratio was 65:20:15 in all panels.

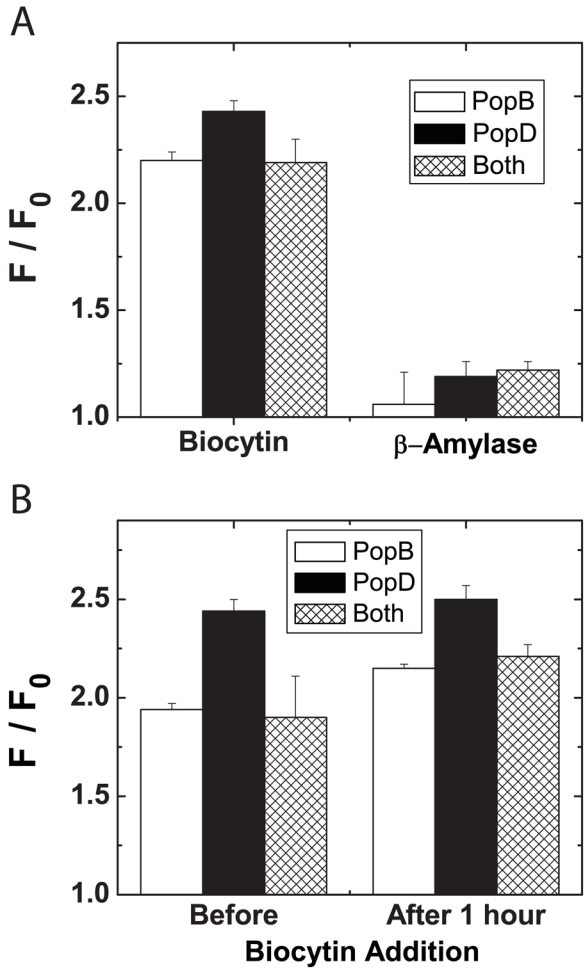

Figure 5. PopD and PopB form discrete and stable pores in model membranes

(A) The passage of biocytin (~10Å diameter), biotin-labeled β-amylase (~50Å diameter), or streptavidin-Bodipy (~50Å diameter) through the pores formed by PopD, PopB, or an equimolar mixture of the translocators was measured as detailed in experimental procedures. Total lipid concentration was 100 μM, and protein concentration of the proteins was 100 nM (protein:lipid ratio was 1/1000 for individual proteins and 1/500 when added together). The fluorescence intensity of encapsulated streptavidin-Bodipy was measured before (F_0) or after the incubation for 60 min at 25°C with the translocators (F). Only biocytin was able to diffuse through the formed pores. (B) The stability of the formed pores was examined by measuring the increase on the fluorescence intensity of encapsulated streptavidin-Bodipy when biocytin was present in the external buffer solution before the addition of the translocators, or added after 1 hr of incubation with the translocators. The discrete pores formed by PopB, PopD, and an equimolar mixture of the proteins remained open after1hr of incubation.

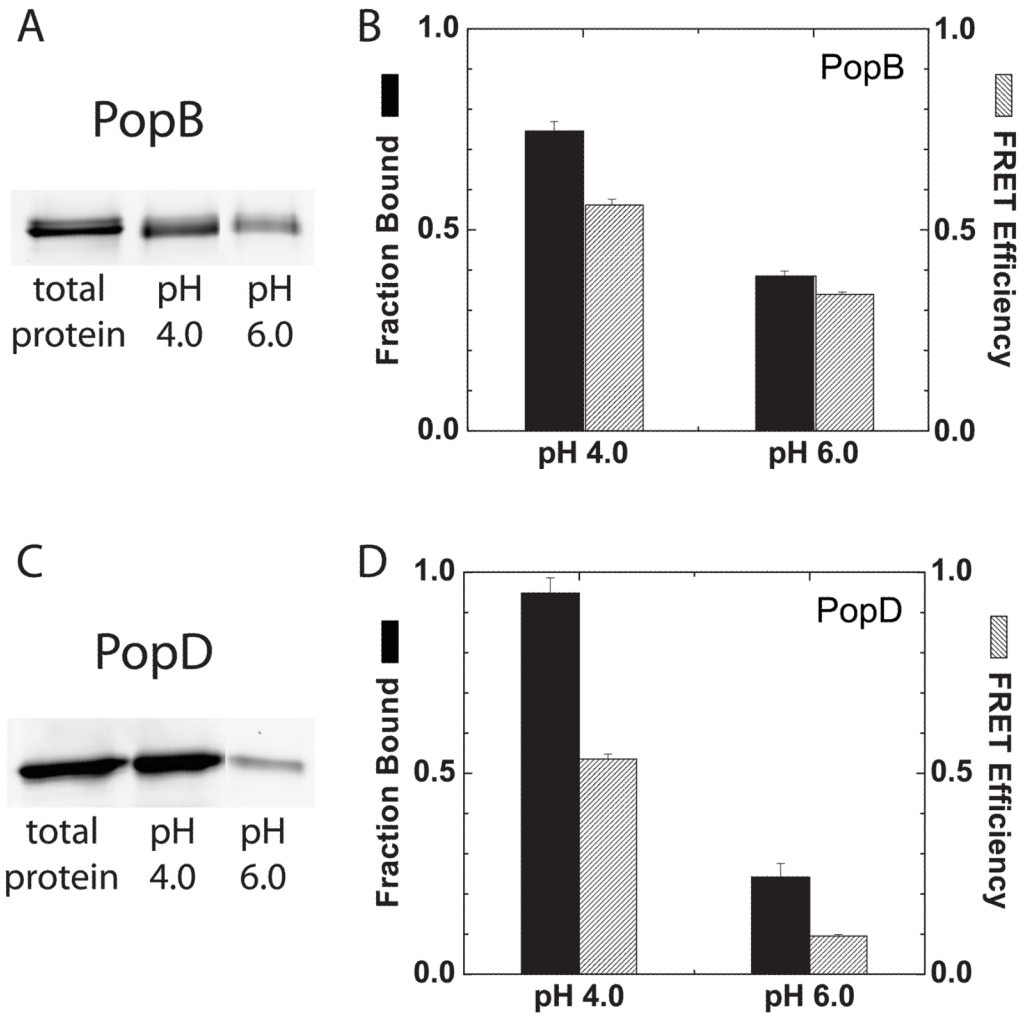

Figure 6. Acidic pH enhances translocator membrane binding

(A) PopB$^{S164C\text{-}Bodipy}$ membrane binding was measured using the liposome floatation assay described in experimental procedures. PopB$^{S164C\text{-}Bodipy}$ (0.4 μM) was incubated with membranes (2 mM total lipids) for 1 hr at 20–23°C. Typical SDS-PAGE analysis is indicated showing the amount of total protein added, and the amount of bound protein isolated after incubation with membranes at the indicated pH. Protein:lipid ratio was 1:5000. Gels were scanned for Bodipy fluorescence using a phosphoimager. (B) Quantification of PopB$^{S164C\text{-}Bodipy}$ binding measured by liposome floatation assay (Fraction Bound, black bars). Data was normalized against the total amount of protein used in the binding reaction. Each bar represents the average and range of at least two independent experiments. FRET efficiency (grey bars) for PopB$^{S164C\text{-}Bodipy}$ binding determined by time-resolved FRET as described in experimental procedures. PopB$^{S164C\text{-}Bodipy}$ (120 nM) was incubated with membranes (total lipid concentration 0.3 mM) as described in A) (protein:lipid ratio was 1:2500). Each bar represents the average and range of two independent experiments. (C) and (D) show the analysis for PopD$^{F223C\text{-}Bodipy}$ binding as described in A) and B) for PopB$^{S164C\text{-}Bodipy}$. The POPC:cholesterol:POPS molar ratio was 65:20:15 in all panels.

Table 1

Bodipy detected protein-protein interaction in intact membranes

Relative fractions of proteins added are indicated. Labeled and unlabeled proteins were mixed in buffer B supplemented with 6 M urea and 20 mM Gly solution previous to dilution in buffer D in the presence of membranes. The final fluorescence parameters measured for the different samples are indicated: I, fluorescence emission intensity; I_{10}/I_{100}, the ratio of the fluorescence emissions of diluted over undiluted labeled protein sample; $\langle\tau\rangle_{\alpha}$, the amplitude weighted average fluorescence lifetimes. The fluorescence lifetime of Bodipy in sodium acetate 50 mM, pH 4.0 was 5.85 ns. The fluorescence lifetime of monomeric $PFO^{C459A\ E167C\text{-}Bodipy}$ in buffer C was 5.51 ns. Labeling efficiencies were 100%, 96%, and 68% for $PFO^{C459A\ E167C\text{-}Bodipy}$, $PopD^{F223C\text{-}Bodipy}$, $PopB^{S164C\text{-}Bodipy}$, respectively. The average and range of at least two determinations are shown. Protein:lipid ratios were 1:2500 for fluorescence lifetimes and 1:10000 for steady state determinations.

Fraction of protein added		I	I_{10}/I_{100}	r	$\langle\tau\rangle_{\alpha}$[a]
PFO^{Bodipy}	PFO	Relative units			ns
1	-	1.84 ± 0.09		0.050 ± 0.005	1.55 ± 0.01
1	9	8.27 ± 0.07	4.5 ± 0.2	0.123 ± 0.005	4.75 ± 0.01
$PopD^{Bodipy}$	PopB				
1	-	6.5 ± 0.2		0.161 ± 0.004	2.56 ± 0.03
1	9	14.4 ± 0.2	2.22 ± 0.08	0.186 ± 0.009	3.90 ± 0.03
$PopB^{Bodipy}$	PopD				
1	-	4.32 ± 0.04		0.185 ± 0.003	3.24 ± 0.02
1	9	7.1± 0.2	1.63 ± 0.02	0.226 ± 0.003	4.93 ± 0.04

[a] Time-resolved fluorescence data for 10% labeled PFO best fit to a single exponential component. The remaining data presented best fit to a two-exponential component (See Table S1).